Contribution of the vibration of various piano components in the resulting piano sound

ICA 2016 BUENOS AIRES
Buenos Aires – 5 to 9 September 2016
Acoustics for the 21st Century...

PROCEEDINGS of the 22nd International Congress on Acoustics

String Instruments: Paper ICA2016-171

Contribution of the vibration of various piano components in the resulting piano sound

Jin Jack Tan[(a)(b)], **Antoine Chaigne**[(b)], **Antonio Acri**[(c)(d)]

[(a)]IMSIA-ENSTA-ParisTech-CNRS-EDF-CEA, France, jtan@ensta.fr
[(b)]University of Music and Performing Arts Vienna, Austria, chaigne@mdw.ac.at
[(c)]Virtual Vehicle (ViF), Austria, antonio.acri@v2c2.at
[(d)]Politecnico di Milano, Italy, antonio.acri@polimi.it

Abstract

To date, piano sound modelling is focused primarily on the vibrational behaviour of the strings and soundboard. However, it is observed that other components of piano such as the rim also vibrate when the piano is being played. Current work serves as a pilot experimental investigation on the contribution of the vibration of various components of the piano to the resulting piano sound. The components inspected are the soundboard, the inner and outer rim, the cast-iron frame and the lid. Vibrations of the components are captured by accelerometers and in parallel, sound pressure is recorded by microphones. Operational transfer path analysis is conducted to identify the main contributors of the sound.

Keywords: piano radiation, structural acoustics, operational transfer path analysis

Contribution of the vibration of various piano components in the resulting piano sound

1 Introduction

To create a realistic sound for piano synthesis, the physics of the piano strings and soundboard are studied and numerical models of them are built [1–3]. Other components like the bridge [4] and the action [5] are also investigated as these components contribute to the modeling of piano sound. However, when a piano is played, other components like the inner rim, the outer rim, the frame and the lid also vibrate. The contribution of these vibrations to the resulting piano sound, if any, is not known nor studied. To find out their contributions, an experimental investigation is carried out on a grand piano to study the aforementioned components. The vibrations are measured at discrete points all over the piano and the relationship between these vibrations and the resulting piano sound is studied.

Current work takes inspiration of noise source identification techniques used commonly in automotive acoustics [6]. However, in the case of piano, the "noise" is the resulting piano sound and the "sources" to be identified are the piano components to be investigated. These "sources" may emit different "noise" contributions that characterise the resulting "noise", i.e. the piano sound. One technique that can be used to identify the contribution of the piano components to the final sound is the operational transfer path analysis (OTPA) [7]. OTPA computes a transfer function matrix to relate a set of input(s) measurements to output(s) measurements. In this case, the inputs are the vibration of the components of piano and the output is the resulting piano sound. A detailed presentation of OTPA is explained in Section 2. The experimental setup to fulfill the analysis is then presented in Section 3, followed by the results and discussion in Section 4. The paper ends with the conclusion of the finding in Section 5.

2 Theory of OTPA

Operational transfer path analysis (OTPA) is a technique derived from the more established classical transfer path analysis (TPA) [6,8]. TPA traces the flow of vibro-acoustic energy from a source through a set of known structure- and air-borne pathways, to a given receiver location. The excitation intensity and frequency response functions between the sources and receivers are estimated so that the transfer functions of the system can be determined. On the other hand, OTPA computes directly the transfer functions of the system that relates the sources (i.e. the piano components) to the receivers (i.e. the piano sound) using experimental measurements [7]. The measurements are taken in operational condition of the piano where it is played directly from the keys instead of exciting the strings or soundboards via shakers, impact hammers etc. A successful OTPA gives insights on the contribution of each sources to the receivers over the considered frequency ranges by studying the computed transfer functions. In automotive applications, this allows engineers to modify the components to supress or compensate for the noise generated. However, for the interest of current work, knowing the level of contributions of the components in piano can shed light to the necessity in modelling them for

numerical simulation.

In a linear system, the input $\mathbf{X}$ and output $\mathbf{Y}$ can be related by:

$$\mathbf{Y}(j\omega) = \mathbf{X}(j\omega)\mathbf{H}(j\omega) \tag{1}$$

where:
$\mathbf{Y}(j\omega)$ is the output vector/matrix at the receivers;
$\mathbf{X}(j\omega)$ is the input vector/matrix at the sources;
$\mathbf{H}(j\omega)$ is the operational transfer function matrix, also known as the transmissibility matrix.

Given that there are m inputs and n outputs with p set of measurements, equation (1) can be written in the expanded form:

$$\begin{bmatrix} y_{11} & \cdots & y_{1n} \\ \vdots & \ddots & \vdots \\ y_{p1} & \cdots & y_{pn} \end{bmatrix} = \begin{bmatrix} x_{11} & \cdots & x_{1m} \\ \vdots & \ddots & \vdots \\ x_{p1} & \cdots & x_{pm} \end{bmatrix} \begin{bmatrix} H_{11} & \cdots & H_{1n} \\ \vdots & \ddots & \vdots \\ H_{m1} & \cdots & H_{mn} \end{bmatrix} \tag{2}$$

where for brevity purposes, the frequency dependency $j\omega$ is dropped. If $\mathbf{X}$ is not a square matrix, which is the case most of the times, $\mathbf{H}$ can be solved by:

$$\mathbf{H} = \mathbf{X}^{+}\mathbf{Y} \tag{3}$$

where the symbol $+$ denotes the Moore-Penrose pseudo-inverse [9]. For the system to be solvable and accurate, it is required that the number of measurement sets is larger than or equal to the number of inputs, i.e.

$$p \geq m \tag{4}$$

In an OTPA, all measurements are taken simultaneously. As a result, cross-talk between measurement channels is expected. Singular value decomposition (SVD) can be used to prevent poor estimates of the transfer functions [10] and principal component analysis (PCA) can follow to eliminate cross-talk [7, 11]. After applying SVD, the input matrix $\mathbf{X}$ can be written as

$$\mathbf{X} = \mathbf{U}\mathbf{\Sigma}\mathbf{V}^{\mathbf{T}} \tag{5}$$

where
$\mathbf{U}$ is a unitary column-orthogonal matrix;
$\mathbf{\Sigma}$ is a diagonal matrix with the singular values;
$\mathbf{V}^{\mathbf{T}}$ is the transpose of a unitary column-orthogonal matrix, $\mathbf{V}$.
Next, the principal components (PCs) are obtained by multiplying the matrix of the singular values $\mathbf{\Sigma}$ with the eigenvector matrix $\mathbf{U}$

$$\mathbf{Z} = \mathbf{X}\mathbf{V} = \mathbf{U}\mathbf{\Sigma} \tag{6}$$

The smaller contributions in matrix $\mathbf{Z}$ (i.e. cross-talk and measurement noise) correspond to the PCs that can be removed. This yields a modified singular value matrix $\mathbf{\Sigma}_{\boldsymbol{m}}$ which can then be used to obtain the modified pseudo-inverse of $\mathbf{X}$:

$$\mathbf{X}_{\mathbf{m}}^{+} = \mathbf{V}\mathbf{\Sigma}_{\boldsymbol{m}}^{-1}\mathbf{U}^{\mathbf{T}} \tag{7}$$

Introducing equation (7) into equation (3), it is possible to obtain a transmissibility matrix $\mathbf{H_m}$ in which cross-talk terms and noise are treated.

$$\mathbf{H_m} = \mathbf{X_m^+ Y} \tag{8}$$

Lastly, it is possible to synthesise the response contributions of the measurements $\mathbf{Y_s}$ by performing a point-wise multiplication between $\mathbf{X}$ and $\mathbf{H_m}$:

$$\mathbf{Y_s} = \mathbf{X} . \mathbf{H_m} \tag{9}$$

The synthesised response $\mathbf{Y_s}$ is useful to determine the validity of the analysis. On the other hand, the transmissibility matrix $\mathbf{H_m}$ is important to determine the contribution of the sources/inputs (i.e. the piano components) to the receivers/outputs (i.e. the piano sound). These are detailed in Section 4.

3 Experimental setup

Acceleration data of the vibration of various points on a piano and the sound pressure are recorded in an anechoic chamber in the University of Music and Performing Arts Vienna. The experiment is conducted on a Bösendorfer 280VC-9 equipped with a CEUS Reproducing System. There are two microphones: #1 placed outside the piano, and #2 inside the piano as shown in Figure 1 and as detailed in Table 1. The accelerometers are placed on these piano components: the soundboard, the inner rim, the outer rim, the frame and the lid. Accelerometers are placed with 20cm spacing between each other and a total of 174 points are sampled across all the investigated components. For the analysis, the sound pressure signals obtained from microphones are considered as the outputs and the acceleration data as the inputs.

As there are only 7 accelerometers available, the measurements have to be made in multiple batches. In order to ensure that all measurements are excited identically, the CEUS system is used. The excitation is coded in a .boe file that can be read by the CEUS system. The .boe file is a file format developed by Bösendorfer and is made up of hexadecimal characters to indicate the keys to play, the key pushing profiles and the hammer velocities. Excitation sequences were made via an in-house MATLAB/GNU Octave script. For this experiment, the file contains 13 sequences of playing, with the first twelve playing all the same notes, starting with all A (i.e. A0, A1, A2 ... A7) and is followed by all A#, all B, all C until all G#. The 13th sequence, however, plays all 88 notes. Each sequence is played for 5 seconds with 1 second interval in between and at a moderate piano velocity that gives a subjective loudness of *mezzoforte*.

4 Results and discussion

By conducting a comprehensive sampling over each piano components, all of the vibrational modes can be captured and be analysed via operational transfer path analysis (OTPA). However, in order to carry out the analysis, equation (4) needs to be satisfied, i.e. the number of

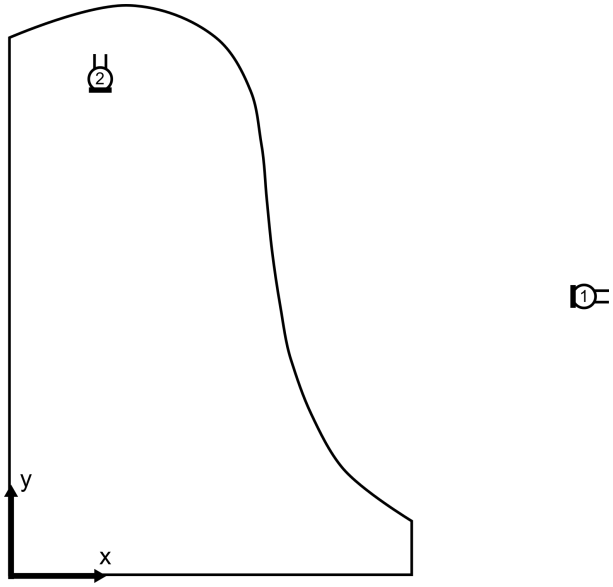

Figure 1: **Location of the two microphones with respect to the outline of the piano soundboard. The image is to scale.**

Table 1: **Location of the microphones with the coordinate axes as shown in Figure 1. *z*=0 indicates the point is on the plane of the soundboard.**

Microphone	1	2
x (m)	2.2	0.4
y (m)	1.0	1.8
z (m)	0.0	0.2

inputs cannot exceed the number of excitations. To reduce the number of inputs, the acceleration distribution data are summed using the Rayleigh integral. The net pressure radiated at a coordinate in space can be described by equation (10):

$$p(\mathbf{R},\omega) = \frac{\rho}{2\pi}\sum_{n=1}^{N}\frac{A_n S_n}{\mathbf{r_n}}e^{-jk\mathbf{r_n}} \tag{10}$$

where ρ is the density of air, A_n, $\mathbf{r_n}$, k and S_n represent the acceleration, distance to the summed point, wavenumber and area covered of source point n respectively. A similar form but expressed in velocity field and displacement field can be found in reference texts like Cremer, Heckl and Petersson [12], and Chaigne and Kergomard [13] respectively. This summation is illustrated in Figure 2 for three example source points on the soundboard A_1, A_2 and A_3 with displacements of $\mathbf{r_1}$, $\mathbf{r_2}$ and $\mathbf{r_3}$ respectively to the microphone location #1.

The use of equation (10) is essentially a compromise as it is valid for an infinitely large baffle.

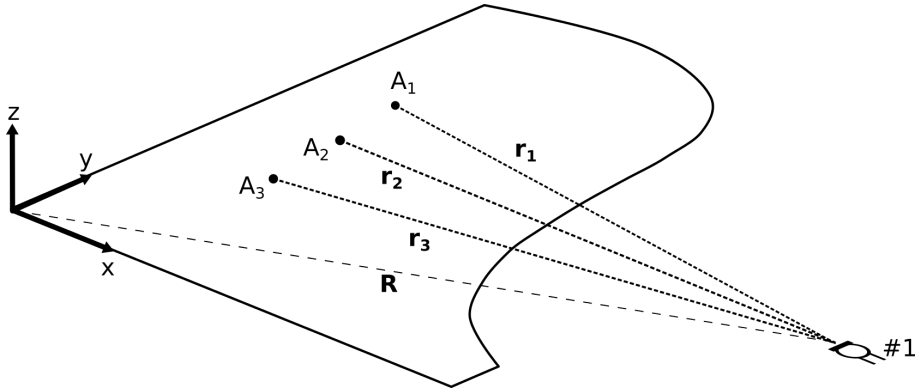

Figure 2: **Summation of point sources A_1, A_2 and A_3 to microphone location #1.**

While the soundboard and lid have a nominal length of about 1.47m, acoustical short circuit could still occur for wave modes below 230Hz. This leads to overestimation of the calculated pressure. For components like the inner and outer rim, the surface area is smaller and thus the overestimation frequency limit would be higher, at approximately 2000Hz. Last but not least, even though the frame has a complex shape, for simplicity of calculation, the area of the frame is taken to be the same as the soundboard. This implies that the overestimation limit is also at 230Hz. Nonetheless, despite the overestimation, the analysis of the data are not compromised. Current work is interested in the contribution of the components in comparison to one another. Thus, absolute values are not that important.

In this experiment, the input matrix $\mathbf{X}$ is made up of five signals, i.e. $m = 5$. The acceleration data of each component is summed up to be pressure using equation (10). The pressure is radiated to where the microphone is located at as is shown as an example in Figure 2. For each analysis, there is only one output $\mathbf{Y}$, i.e. $n = 1$. The output is the sound pressure signal received by the microphone. OTPA is first conducted with the sound samples from microphone #1 and is then repeated with samples from microphone #2.

The first step of the analysis is to validate the transmissibility matrix $\mathbf{H_m}$. This can be achieved by comparing the actual experimental output $\mathbf{Y}$ to the synthesised sound pressure output $\mathbf{Y_s}$, as obtained via equation (9). Figure 3 shows the frequency responses of the synthesised and measured sound pressure at microphone location #1 when all the A notes are being played. It can be seen that the synthesised pressure matches closely with the actual measurement. It correctly identifies the partials up to 880Hz and at similar amplitude. Good agreements are also seen throughout the frequency range for the other excitations but are omitted for brevity. This suggests that the transmissibility matrix $\mathbf{H_m}$ is accurate and passes the validation test.

Next, the contributions to output #1 (microphone outside the piano) of each components are analysed. In Figure 4, the average contribution of the components of five frequency ranges are shown. These five frequency ranges correspond to the first 5 octaves in the piano scale. The first 5 bars in each block correspond to the 5 components investigated, i.e. the soundboard, inner rim, outer rim, frame and lid. The 6th bar is the sum of all of these components and

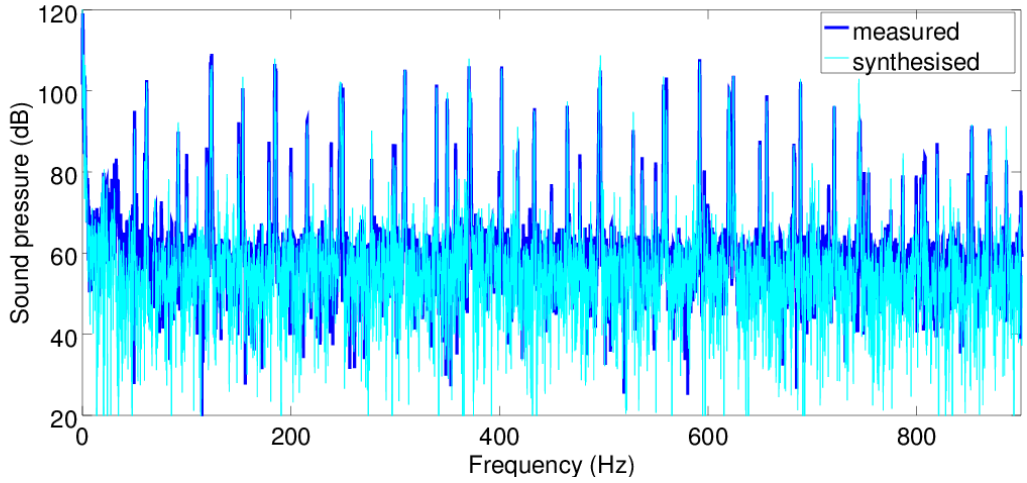

Figure 3: **Frequency responses of the synthesised and the measured sound pressure at output #1 when excited by playing all A notes.**

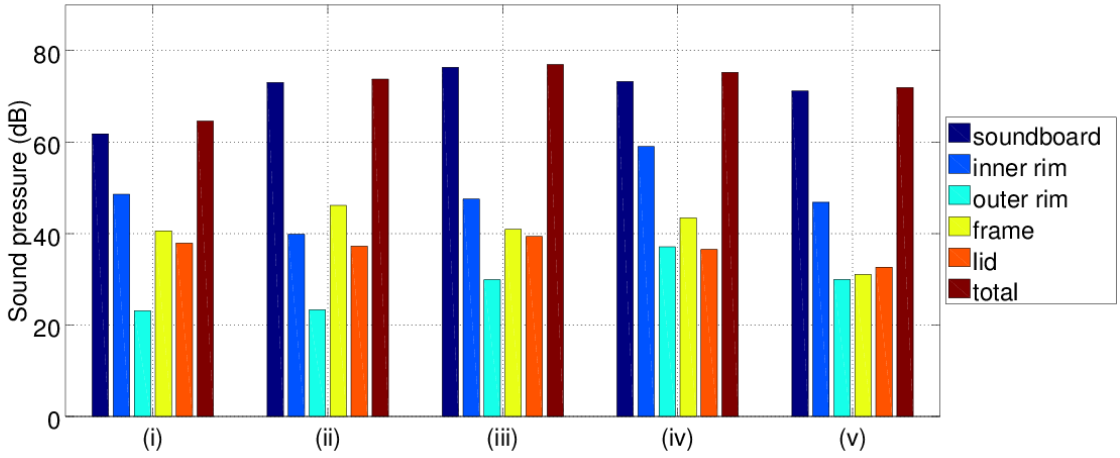

Figure 4: **Contribution of the components at output #1 in the frequency range (i) 27.5Hz to 55Hz, (ii) 55Hz to 110Hz, (iii) 110Hz to 220Hz, (iv) 220Hz to 440Hz, and (v) 440Hz to 880Hz.**

represent the synthesised output summed for all measurement sets. It is interesting to note that when comparing this value to the corresponding measured summed output, the measured amplitude turns out slightly higher by 1-2dB than the synthesised amplitude (not shown in Figure 4 for better presentation of key data). This is despite that the synthesised output is being overestimated by Rayleigh integral summation. This small discrepancy could be due to the noise removal by the principal component analysis as detailed from equation (6) to equation (7). Nonetheless, the small discrepancy also suggests that all of the significant modes are captured and properly considered by the OTPA.

Figure 4 shows that soundboard is the primary contributor for all frequency ranges considered, followed by inner rim. Except for frequency range (ii), inner rim is the second highest contributor, most notably at (i) and (iv) where it is about 13dB weaker than the soundboard. At other instances, the inner rim is about 20-30dB less than the soundboard. On the other hand, the frame and lid have comparable contribution and they contribute less than the inner rim except at (ii) where the frame is stronger than the inner rim. The contribution of these two components are noticeably higher than the outer rim but decreases at higher frequencies until they are all comparable at (v). The outer rim has very weak contribution at lower frequency range from (i) to (iii).

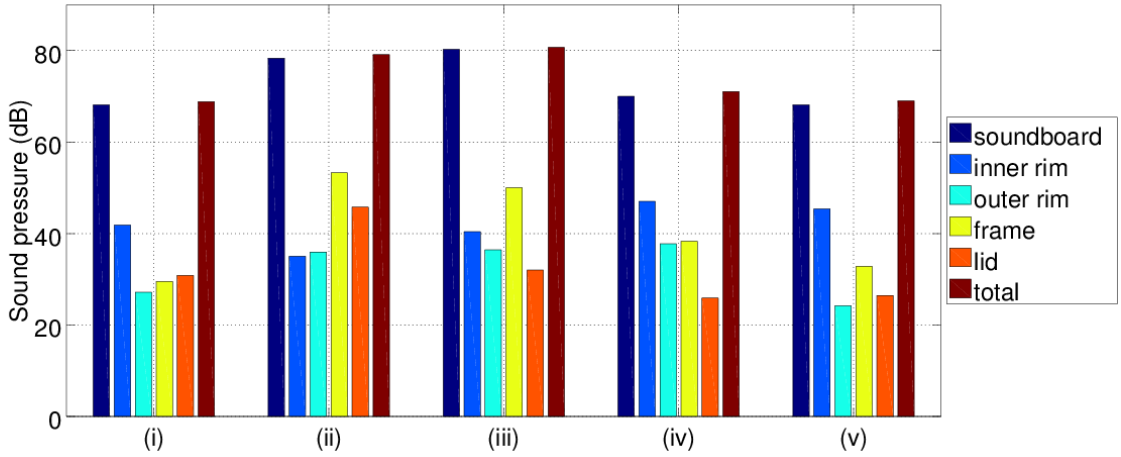

Figure 5: **Contribution of the components at output #2 in the frequency range (i) 27.5Hz to 55Hz, (ii) 55Hz to 110Hz, (iii) 110Hz to 220Hz, (iv) 220Hz to 440Hz, and (v) 440Hz to 880Hz.**

The analysis is repeated for output #2 and the result is shown in Figure 5. The result is similar to Figure 4 but with a few differences. Soundboard is unsurprisingly the main contributor, followed by the inner rim. However, the inner rim contribution is lesser as it is at least about 20dB weaker than the soundboard. At frequency range (ii) and (iii), frame contributes the most after the soundboard. At frequency range (ii), the lid becomes the third highest contributor while inner rim contributes the least. The increase of contribution from the frame and lid at (ii) and (iii) could be attributed to the proximity of the microphone placement to these components. At these frequency ranges, the outer rim is also comparable to inner rim and at other instances, it is comparable to the frame or lid. The overall contribution of outer rim is not significant.

The reason why soundboard is the main contributor can be explained in Figure 6. The frequency responses of each of the inputs and output #1 from 300Hz to 340Hz are shown and there are 2 notes in this frequency range, namely D#4 (311.1Hz) and E4 (329.6Hz). It can be seen that at these two frequencies, all components are excited. However, the amplitude varies between the components but all other components are weaker than the soundboard. Other than that, there are additional peaks (e.g. at 302.9Hz, 305.4Hz and at 320.5Hz). Only the soundboard is excited at these modes which are also found in the resulting sound. These are

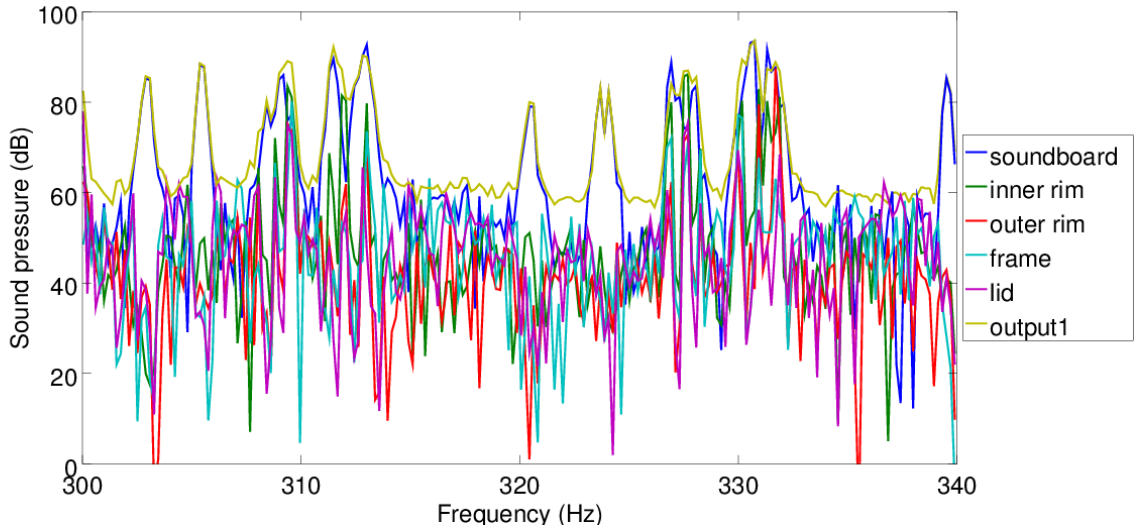

Figure 6: **Contribution of the components in the frequency range 300Hz to 340Hz.**

either the soundboard modes or phantom partials that arise due to nonlinearity. Similarly, at other frequency range, the soundboard has the largest amplitude and is also present at additional frequency peaks. These result in soundboard being the main contributor by a margin compared to the other components.

Meanwhile, the contribution of the inner rim is not to be ignored. The inner rim is the second highest contributor after the soundboard in frequency range (i), (iii), (iv) and (v) for output #1 and in frequency range (i), (iv) and (v) for output #2. The contribution of inner rim can be explained intuitively. The edges of soundboard are in contact with the inner rim and the contact can represent a path for the soundboard to lose energy to. Subsequently, the rim vibrates and contribute to the sound. In addition to that, it may also be due to the unique construction of the Bösendorfer piano, which uses spruce for the rim instead of multiple layers of hard woods. For these reasons, it may be worthwhile to model the vibration of inner rim in a numerical simulation of piano.

5 Conclusions

Operational transfer path analysis (OTPA) is implemented to investigate the main contributors of the sound of a Bösendorfer 280VC-9 piano. The analysis shows that the soundboard contributes the most to the overall sound, followed by the inner rim. At low frequency ranges, the frame and the lid play a role as well. Conversely, outer rim is the least influential overall.

Acknowledgements
The research work presented in this paper is funded by the European Commission within the Initial Training Network (ITN) Marie Skłodowska Curie action BATWOMAN project, under the

seventh framework program (EC grant agreement no. 605867). The authors thank the project for the generous funding and support.

References

[1] Chabassier, J.; Chaigne, A.; Joly, P. Modeling and simulation of a grand piano. The Journal of the Acoustical Society of America, 134(1), 2013, pp.648-665.

[2] Bilbao, S. Conservative numerical methods for nonlinear strings. The Journal of the Acoustical Society of America, 118(5), 2005, pp.3316-3327.

[3] Giordano, N. Simple model of a piano soundboard. The Journal of the Acoustical Society of America, 102(2), 1997, pp.1159-1168.

[4] Ege, K.; Chaigne, A. End conditions of piano strings. arXiv preprint arXiv:1101.4511, 2011. (available at: https://arxiv.org/ftp/arxiv/papers/1101/1101.4511.pdf)

[5] Chabassier, J; Duruflé, M. Energy based simulation of a Timoshenko beam in non-forced rotation. Influence of the piano hammer shank flexibility on the sound. Journal of Sound and Vibration, 333(26), 2014, pp.7198-7215.

[6] Plunt, J. Finding and fixing vehicle NVH problems with transfer path analysis. Sound and vibration, 39(11), 2005, pp.12-17.

[7] Toome, M. Operational transfer path analysis: A study of source contribution predictions at low frequency. Master's Thesis, Chalmers University of Technology, Sweden, 2012.

[8] van der Seijs, M.V.; de Klerk, D; Rixen, D.J. General framework for transfer path analysis: History, theory and classification of techniques. Mechanical Systems and Signal Processing, 68, 2016, pp.217-244.

[9] Penrose, R. A generalized inverse for matrices. Mathematical Proceedings of the Cambridge Philosophical Society, 51(3), 1955, pp.406-413

[10] De Klerk, D.; Ossipov, A. Operational transfer path analysis: Theory, guidelines and tire noise application. Mechanical Systems and Signal Processing, 24(7), 2010, pp.1950-1962.

[11] Jolliffe I. Principal component analysis. Springer-Verlag, New York (USA), 2nd edition, 2002.

[12] Cremer, L.; Heckl, M; Petersson, B.A.T. Structure-borne sound structural vibrations and sound radiation at audio frequencies. Springer-Verlag, Berlin (Germany), 3rd edition, 2013.

[13] Chaigne, A.; Kergomard, J. Acoustics of Musical Instruments. Springer-Verlag, New York (USA), 2016.